East Asian Journal on Applied Mathematics
doi: 10.4208/eajam.2023-004.200423

Vol. **14**, No. 1, pp. 79-103
February 2024

# Numerical Methods for the Nonlinear Dirac Equation in the Massless Nonrelativistic Regime

Ying He[1,2], Yan Wang[3,*], Jerry Zhijian Yang[1] and Hongshuang Yin[1]

[1]*School of Mathematics and Statistics, Wuhan University, Wuhan 430072, P.R. China.*
[2]*Yanqi Lake Beijing Institute of Mathematical Sciences and Applications, Beijing, 101408, P.R. China.*
[3]*School of Mathematics and Statistics and Hubei Key Laboratory of Mathematical Sciences, Central China Normal University, Wuhan 430079, P.R. China.*

*Received 4 January 2023; Accepted (in revised version) 20 April 2023.*

**Abstract.** Numerical methods for the nonlinear Dirac equation (NDE) in the massless nonrelativistic regime are considered. In this regime, the equation contains a small dimensionless parameter $0 < \varepsilon \leq 1$, and its solution is highly oscillatory in time. We present and analyze traditional numerical schemes for the NDE, including finite difference methods, time-splitting methods and exponential integrators. Error analysis indicates that all these methods require an $\varepsilon$-dependent time-step size to achieve an optimal convergence order. Utilizing an operator splitting technique, we propose a uniformly accurate (UA) scheme. The scheme enables first-order convergence in time for all $\varepsilon \in (0, 1]$ without restrictions on time-step size. Error estimates for the UA scheme are rigorously established and numerical results confirm the properties of the method.

**AMS subject classifications**: 35Q41, 65M12, 65M70

**Key words**: Nonlinear Dirac equation, uniformly accurate, finite difference method, time-splitting method, exponential integrator.

## 1. Introduction

The equation derived by Paul Dirac [21, 22] for describing spin-1/2 massive particles was named after him. It plays an important role in particle physics and relativistic quantum mechanics since then. It predicts the existence of positrons, and it is consistent with both the principle of quantum mechanics and the theory of special relativity. Later on, in 1938, Ivanenko [30] introduced a nonlinear Dirac equation by taking into account the self-interaction of particles. It has received considerable attention in mathematical and

*Corresponding author. *Email addresses:* heymath@whu.edu.cn (Y. He), wang.yan@ccnu.edu.cn (Y. Wang), zjyang.math@whu.edu.cn (Z. Yang), 2019202010048@whu.edu.cn (H. Yin)

 

physical studies [25,31], especially on solitary wave solutions [2,28,39,46]. Recently, the Dirac equation and the NDE attract renewed interests since they can be adopted to study graphene and Bose-Einstein condensates [1,23,26].

In this work, we consider the following one-dimensional NDE [5,7,10,21,22] on a torus $\mathbb{T} = \mathbb{R}/(2\pi)$ with periodic boundary conditions:

$$\begin{aligned} i\hbar\partial_t u(t,x) &= -ic\hbar\alpha\partial_x u(t,x) + mc^2\beta u(t,x) \\ &\quad + eVu(t,x) + F\big(u(t,x)\big), \quad t>0, \quad x\in\mathbb{T}, \\ u(0,x) &= u_0(x), \qquad\qquad\qquad\qquad\qquad\quad x\in\mathbb{T}, \end{aligned}$$

where

$$u := u(t,x) = \big(u_1(t,x), u_2(t,x)\big)^T : [0,+\infty)\times\mathbb{T}\to\mathbb{C}^2$$

is the complex-valued vector wave function of the spinor field, $V := V(x)$ the real-valued electrical potential, $\hbar$ the Planck constant, $c$ the speed of light, $m$ the mass, and $e$ the unit charge. We take the nonlinearity as $F(u) = \lambda(u^*\beta u)\beta u$ with $\lambda\in\mathbb{R}$ denoting the strength of the nonlinear interaction [43] and $u^* = \overline{u}^T$, while $\overline{u}$ denotes the complex conjugate of $u$, and $\alpha,\beta$ are the Pauli matrices

$$\alpha = \begin{pmatrix} 0 & 1 \\ 1 & 0 \end{pmatrix}, \quad \beta = \begin{pmatrix} 1 & 0 \\ 0 & -1 \end{pmatrix}.$$

Using the nondimensionalization

$$\tilde{x} = \frac{x}{x_s}, \quad \tilde{t} = \frac{t}{t_s}, \quad \tilde{V} = \frac{V}{A_s}, \quad \tilde{u} = \frac{u}{u_s},$$

where $x_s$, $t_s = m_s x_s^2/\hbar$, $A_s = m_s x_s^2/et_s^2$, $u_s = x_s^{-1/2}$ and $m_s$ are respectively dimensionless length, time, potential, spinor field, and mass units — cf. [4, 5], and removing tilde $\tilde{}$ everywhere, we arrive at a dimensionless form of the nonlinear Dirac equation — viz.

$$\begin{aligned} i\partial_t u(t,x) &= -i\frac{1}{\varepsilon}\alpha\partial_x u(t,x) + \delta\beta u(t,x) \\ &\quad + Vu(t,x) + F\big(u(t,x)\big), \quad t>0, \quad x\in\mathbb{T}, \\ u(0,x) &= u_0(x), \qquad\qquad\qquad\qquad\quad x\in\mathbb{T} \end{aligned} \tag{1.1}$$

with $\delta = m_0/\varepsilon^2$. Note that $0<\varepsilon, m_0\le 1$ the dimensionless parameters defined by

$$\varepsilon := \frac{x_s}{t_s c} = \frac{v_s}{c}, \quad m_0 := \frac{m}{m_s},$$

where $v_s = x_s/t_s$ is the dimensionless velocity unit, $\varepsilon$ the ratio between the wave velocity and the speed of light — i.e. it is inversely proportional to the speed of light, and $m_0$ the ratio between the mass of the particle $m$ and the dimensionless mass unit $m_s$.

Under different scaling, the Eq. (1.1) corresponds to different parameter regimes, including the standard (classical) regime ($\varepsilon = m_0 = 1$), the nonrelativistic regime ($m_0 =$

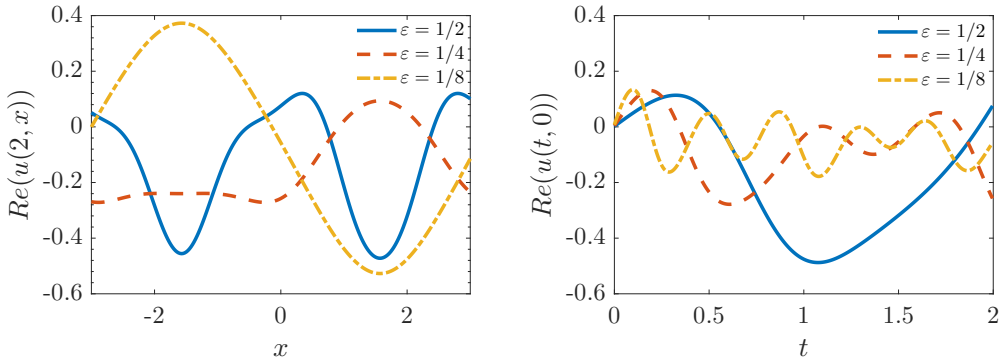


Figure 1: Real part of wave functions $u(2,x)$ and $u(t,0)$ for the Dirac equation (1.1) for various $\varepsilon$.

$1, 0 < \varepsilon \ll 1$), the massless regime ($\varepsilon = 1, 0 < m_0 \ll 1$), and the simultaneously massless and nonrelativistic regime ($0 < \varepsilon, m_0 \ll 1$). There are extensive theoretical and numerical studies of nonlinear and linear Dirac equations in these regimes — cf. [3–6, 10, 13–15, 24, 33, 34, 42, 45] and references therein.

In this paper, we mainly consider the massless nonrelativistic regime — i.e. the situation where $\delta = \mathcal{O}(1)$ ($m_0 = \mathcal{O}(\varepsilon^2)$), $0 < \varepsilon \ll 1$. In this regime, the mass of the particle is much smaller than the mass unit, the wave speed is much smaller than the speed of light, and the NDE (1.1) becomes a highly oscillatory dispersive partial differential equation [10]. More precisely, the solution to (1.1) is highly oscillatory in time and also propagates rapidly in space. To illustrate this, we show the solution in Fig. 1 with $\delta = 1$, $V(x) = 2\sin(x)$ and initial data

$$u_0(x) = \left( \frac{\sin(x)}{2 + \cos(x)^2}, \frac{\cos(x)}{2 + \sin(x)} \right)^T, \quad x \in \mathbb{T} = (-\pi, \pi)$$

for various $\varepsilon$.

It is well known that the highly temporal oscillation brings severe burdens to numerical computation [7, 14] i.e. the time-step size (or even the mesh size) of a numerical method is mostly restricted to be smaller than the oscillatory wavelength. Otherwise, the method is unable to capture the oscillation and loses its accuracy. To enhance the computational efficiency and stability in real applications, it is necessary to develop a uniformly accurate method, which resolves the solution without restrictions on the time-step and mesh sizes. Recently, several kinds of UA methods have been designed for solving highly oscillatory equations [8, 9, 11, 17, 19, 20]. The multiscale time integrator and the exponential-type integrator with twisted variables both rewrite the equation to new systems without dominant oscillation. The former adopts a multiscale expansion of the solution [8, 9], and the latter utilizes twisted variables [17, 19]. The two-scale method separates a new fast time variable from the original slow time variable [19]. The nested Picard iteration integrator (NPI) explicitly extracts the dominant highly oscillatory phases from the evolution operator [12, 15]. It can be seen that a UA method is usually based on a certain technique to exactly deal with the (leading-order) highly oscillatory phases. However, once the equation

changes, these techniques either vanish or usually need to be modified. Thus, each highly oscillatory equation poses a new challenge in designing UA methods.

At present, there are various numerical methods for the NDE. However, to the best of our knowledge, only a few studies study their performance in the massless nonrelativistic regime. Therefore, one aim of this work is to analyze the meshing strategy requirements of traditional numerical methods for the NDE (1.1) in the massless nonrelativistic regime, including finite difference time domain, time-splitting, and exponential integrator methods. It is shown that all these methods have to satisfy meshing strategy restrictions and become less efficient if $0 < \varepsilon \ll 1$.

We also introduce and analyze a UA method for the NDE in the massless nonrelativistic regime. The UA method is constructed by modifying the NPI method for the Dirac equation and the NDE in the nonrelativistic regime [15,16]. The main novelty of this scheme is the choice and splitting of the evolution operator. In the nonrelativistic regime [15,16], the free Dirac operator $\mathscr{T}^\varepsilon := (-i\varepsilon\alpha\partial_x + \beta)/\varepsilon^2$ is chosen to be the linear operator for constructing the integral equation. After that, the (leading-order) highly oscillatory phases $e^{\pm it/\varepsilon^2}$ can be explicitly extracted from the evolution operator $e^{i\mathscr{T}^\varepsilon t}$ due to the following identity:

$$e^{i\mathscr{T}^\varepsilon t} = e^{it/\varepsilon^2} e^{i\mathscr{A}^\varepsilon t}\Pi_+^{\mathscr{T}^\varepsilon} + e^{-it/\varepsilon^2} e^{-i\mathscr{A}^\varepsilon t}\Pi_-^{\mathscr{T}^\varepsilon},$$

where

$$\mathscr{A}^\varepsilon = \frac{\sqrt{Id - \varepsilon^2\partial_{xx}} - Id}{\varepsilon^2}$$

is a bounded operator for all $\varepsilon \in (0,1]$, and $\Pi_\pm^{\mathscr{T}^\varepsilon}$ are defined by

$$\Pi_\pm^{\mathscr{T}^\varepsilon} = \frac{1}{2}\Big[Id \pm \varepsilon^2\big(Id - \varepsilon^2\partial_{xx}\big)^{-1/2}\mathscr{T}^\varepsilon\Big]$$

with the identity operator $Id$. Thus, UA schemes can be generated with exact integration for the highly oscillatory phases. However, the above approach can not be directly adopted in the massless nonrelativistic regime, since the free Dirac operator changes to $-i\alpha\partial_x/\varepsilon + \delta\beta$ with $\delta = \mathscr{O}(1)$ and the above identity vanishes. Interestingly, we found that the operator $\alpha\partial_x$ enjoys a nice diagonalization form — viz.

$$\alpha\partial_x = \partial_x\Pi_+ - \partial_x\Pi_-, \tag{1.2}$$

where

$$\Pi_+ = \frac{1}{2}\begin{pmatrix} 1 & 1 \\ 1 & 1 \end{pmatrix}, \quad \Pi_- = \frac{1}{2}\begin{pmatrix} 1 & -1 \\ -1 & 1 \end{pmatrix}.$$

Therefore, we take $-i\alpha\partial_x/\varepsilon$ as the linear operator and apply the Duhamel's principle. Using the nested Picard iteration and the evolution operator splitting

$$\mathrm{e}^{s\alpha\partial_x/\varepsilon} = \mathrm{e}^{s\partial_x/\varepsilon}\Pi_+ + \mathrm{e}^{-s\partial_x/\varepsilon}\Pi_-, \tag{1.3}$$

we can calculate all integral terms explicitly and exactly. Thus, we obtain a UA scheme for the NDE (1.1), without restrictions on parameter $\varepsilon$ or time-step size. Numerical experiments and comparisons with finite difference, time-splitting, and exponential integrator methods demonstrate the efficiency and advantage of the UA scheme proposed.

The rest of the paper is organized as follows. In Sections 2-4, we analyze the meshing strategy for finite difference, time-splitting, and the exponential integrator methods for the NDE (1.1) in the massless nonrelativistic regime. Section 5 is devoted to the derivation and analysis of the UA scheme. Numerical results are reported in Section 6 and conclusions are drawn in Section 7.

We remark that this work focuses on time integrations, so that all the numerical methods are presented in a semi-discretized form (in time). Besides, we only analyze the local truncation error in time. The detailed error analysis with spatial discretizations is beyond the scope of this work. In this work, we adopt standard notations of Sobolev spaces. Denote

$$H_p^m(\mathbb{T}) = \left\{u \mid u \in H^m(\mathbb{T}),\ \partial_x^l u \ \text{ is periodic on } \ \mathbb{T},\ l = 0, \ldots, m-1\right\},$$
$$W_p^{m,\infty}(\mathbb{T}) = \left\{u \mid u \in W^{m,\infty}(\mathbb{T}),\ \partial_x^l u \ \text{ is periodic on } \ \mathbb{T},\ l = 0, \ldots, m-1\right\}$$

for $m \in \mathbb{N}$ and

$$L^\infty(I;S) = \left\{u(t,x) \mid \max_{t\in I} \|u(t,\cdot)\|_S < \infty\right\}.$$

Let $0 < T < T_{\max} < \infty$ with $T_{\max}$ being the maximal existence time (uniform in $\varepsilon \in (0,1]$) for the solutions to the NDE (1.1). We make the following assumptions for the electrical potential and the exact solution $u := u(t) = u(t,x)$ to the NDE (1.1)

(A) $\|V\|_{W_p^{q_0,\infty}} \le C$,

(B) $\|u\|_{L^\infty([0,T];(H_p^{q_0})^2)} \le C, \quad \|\partial_t u\|_{L^\infty([0,T];(H_p^{q_0-1})^2)} \le \dfrac{C}{\varepsilon}, \quad \|\partial_{tt} u\|_{L^\infty([0,T];(L^2)^2)} \le \dfrac{C}{\varepsilon^2},$

where $C$ is a generic constant, $q_0$ is large enough to satisfy the regularity requirements in space.

## 2. Finite Difference Methods

In this section, we consider two semi-implicit finite difference methods for solving the NDE (1.1), viz.

I. First-order semi-implicit finite difference method (SIFD1)

$$i\frac{u^{n+1}-u^n}{\tau} = -\frac{i}{\varepsilon}\alpha\partial_x u^{n+1} + \delta\beta u^n + Vu^n + F(u^n), \quad n \ge 0. \tag{2.1}$$

II. Second-order semi-implicit finite difference method (SIFD2)

$$\begin{aligned} &i\frac{u^{n+1}-u^{n-1}}{2\tau} = -\frac{i}{\varepsilon}\alpha\partial_x\frac{u^{n+1}+u^{n-1}}{2} + \delta\beta u^n + Vu^n + F(u^n), \quad n \ge 1,\\ &u^1 = u^0 - i\tau\left[-\frac{i}{\varepsilon}\alpha\partial_x u^0 + \delta\beta u^0 + Vu^0 + F(u^0)\right]. \end{aligned} \tag{2.2}$$

Here and in what follows, $\tau = \Delta t > 0$ is the time-step size, $t_n = n\tau$ the time grid, and $u^n := u^n(x) \approx u(t_n, x)$, $0 \le n \le T/\tau$ with the numerical solution $u^0 = u_0(x)$ of the Eq. (1.1). For simplicity, we will omit the spatial variable of time-space functions — e.g. we write $u(t) = u(t, x)$.

Analyzing the local truncation errors of the above methods, we can get a clue to the meshing strategy restrictions. These methods are unconditionally stable and easy to implement. Since what we are concerned with the meshing strategy, we make the methods as simple as possible. They may be different from the ones in [5, 27, 37, 40], although their analysis can be similar. Using the Taylor's expansion

$$u(t_{n+1}) = u(t_n) + \tau \int_0^1 \partial_t u(t_n + s\tau) ds,$$
$$u(t_{n\pm1}) = u(t_n) \pm \tau \partial_t u(t_n) + \tau^2 \int_0^1 (1-s)\partial_t^2 u(t_n \pm s\tau) ds,$$

and the NDE (1.1), we get the truncation error for SIFD1 as

$$\begin{aligned}
\xi^n_{\mathrm{SIFD1}} &:= \frac{i}{\tau}\big[u(t_{n+1}) - u(t_n)\big] + \frac{i}{\varepsilon}\alpha\partial_x u(t_{n+1}) - \delta\beta u(t_n) - Vu(t_n) - F\big(u(t_n)\big) \\
&= \left[ i\int_0^1 \partial_t u(t_n + s\tau) ds - i\partial_t u(t_n) \right] + \frac{i}{\varepsilon}\alpha\big[\partial_x u(t_{n+1}) - \partial_x u(t_n)\big] \\
&\quad + \left[ i\partial_t u(t_n) + \frac{i}{\varepsilon}\alpha\partial_x u(t_n) - \delta\beta u(t_n) - Vu(t_n) - F\big(u(t_n)\big) \right] \\
&= i\tau \int_0^1 (1-s)\,\partial_t^2 u(t_n + s\tau)\, ds + \frac{i\tau}{\varepsilon}\alpha \int_0^1 \partial_t \partial_x u(t_n + s\tau)\, ds,
\end{aligned}$$

and the truncation error for SIFD2 as

$$\begin{aligned}
\xi^n_{\mathrm{SIFD2}} &:= i\frac{u(t_{n+1}) - u(t_{n-1})}{2\tau} + \frac{i}{\varepsilon}\alpha\partial_x \frac{u(t_{n+1}) + u(t_{n-1})}{2} - \delta\beta u(t_n) - Vu(t_n) - F\big(u(t_n)\big) \\
&= i\partial_t u(t_n) + \frac{i}{\varepsilon}\alpha\partial_x u(t_n) - \delta\beta u(t_n) - Vu(t_n) - F\big(u(t_n)\big) \\
&\quad + \frac{i\tau}{2}\int_0^1 (1-s)\big[\partial_t^2 u(t_n + s\tau) - \partial_t^2 u(t_n - s\tau)\big] ds \\
&\quad + \frac{i\tau^2}{2\varepsilon}\alpha \int_0^1 (1-s)\partial_x\big[\partial_t^2 u(t_n + s\tau) + \partial_t^2 u(t_n - s\tau)\big] ds \\
&= \frac{i\tau^2}{2}\int_0^1 \int_{-s}^{s} (1-s)\partial_t^3 u(t_n + w\tau)\, dw ds \\
&\quad + \frac{i\tau^2}{2\varepsilon}\alpha \int_0^1 (1-s)\partial_x\big[\partial_t^2 u(t_n + s\tau) + \partial_t^2 u(t_n - s\tau)\big] ds.
\end{aligned}$$

It follows from assumption (B) that

$$\xi^n_{\mathrm{SIFD1}} = \mathscr{O}\left(\frac{\tau}{\varepsilon^2}\right), \quad \xi^n_{\mathrm{SIFD2}} = \mathscr{O}\left(\frac{\tau^2}{\varepsilon^3}\right),$$

which implies

1. Only with the meshing strategy $\tau \le C\varepsilon^2$, SIFD1 (2.1) can converge at its optimal first-order accuracy.
2. Only with the meshing strategy $\tau \le C\varepsilon^{3/2}$, SIFD2 (2.2) can offer an optimal second-order accuracy.

## 3. Time-Splitting Methods

Now, let us consider the time-splitting methods [32,35]. The methods begin by splitting the NDE (1.1) into two sub-flows — i.e.

$$\begin{aligned} &\Psi^{\mathrm{k}}_t: \quad i\partial_t u = -\frac{i}{\varepsilon}\alpha\partial_x u + \delta\beta u, \quad t>0, \quad x\in\mathbb{T},\\ &\Psi^{\mathrm{p}}_t: \quad i\partial_t u = Vu + F(u), \qquad\quad t>0, \quad x\in\mathbb{T}. \end{aligned}$$

For the above two resulting flows, we have the exact integration

$$\begin{aligned} &\Psi^{\mathrm{k}}_t\big(u(t_0)\big): \quad u(t_0+\tau) = \mathrm{e}^{-i\tau(-i\alpha\partial_x/\varepsilon+\delta\beta)}u(t_0),\\ &\Psi^{\mathrm{p}}_t\big(u(t_0)\big): \quad u(t_0+\tau) = \mathrm{e}^{-i\tau(V\cdot Id+\lambda(|u_1(t_0)|^2-|u_2(t_0)|^2)\beta)}u(t_0), \end{aligned}$$

where $Id$ is the identity operator. Then, the classical first-order Lie-Trotter splitting scheme and the second-order the Strang splitting scheme for solving the NDE (1.1) have the form

$$\text{Lie-Trotter:} \quad u^{n+1} = \Psi^{\mathrm{k}}_\tau \circ \Psi^{\mathrm{p}}_\tau(u^n), \qquad n\ge 0, \tag{3.1}$$

$$\text{Strang:} \quad u^{n+1} = \Psi^{\mathrm{k}}_{\tau/2} \circ \Psi^{\mathrm{p}}_\tau \circ \Psi^{\mathrm{k}}_{\tau/2}(u^n), \quad n\ge 0. \tag{3.2}$$

In the following, we formally analyze their local truncation errors.

### 3.1. Lie-Trotter splitting

For the Lie-Trotter splitting scheme (3.1), the local truncation error is defined as

$$\xi^n := u(t_{n+1}) - \Psi^{\mathrm{k}}_\tau \circ \Psi^{\mathrm{p}}_\tau\big(u(t_n)\big).$$

Applying the Duhamel's formula to (1.1), we have

$$u(t_n+s) = \mathrm{e}^{-is\Gamma}u(t_n) - i\int_0^s \mathrm{e}^{-i(s-w)\Gamma}B^n(w)u(t_n+w)\,dw, \quad 0\le s\le\tau, \quad n\ge 0 \tag{3.3}$$

with $\Gamma := -i\alpha\partial_x/\varepsilon + \delta\beta$ and

$$B^n(w) := V \cdot Id + \lambda\big((u(t_n+w))^*\beta u(t_n+w)\big)\beta.$$

For $s = \tau$ we have

$$u(t_{n+1}) = \mathrm{e}^{-i\tau\Gamma}u(t_n) - i\int_0^\tau \mathrm{e}^{-i(\tau-s)\Gamma}B^n(s)u(t_n+s)\,ds. \tag{3.4}$$

As to $\Psi_\tau^{\mathrm{k}} \circ \Psi_\tau^{\mathrm{p}}(u(t_n))$, by Taylor's expansion, we have

$$\begin{aligned}
&\Psi_\tau^{\mathrm{p}}\big(u(t_n)\big) = \mathrm{e}^{-i\tau B^n}u(t_n) = u(t_n) - i\tau B^n u(t_n) + \xi_1^n,\\
&\Psi_\tau^{\mathrm{k}} \circ \Psi_\tau^{\mathrm{p}}\big(u(t_n)\big) = \mathrm{e}^{-i\tau\Gamma}\Psi_\tau^{\mathrm{p}}\big(u(t_n)\big) = \mathrm{e}^{-i\tau\Gamma}\big(u(t_n) - i\tau B^n u(t_n) + \xi_1^n\big)
\end{aligned}$$

with $B^n := B^n(0)$ and

$$\xi_1^n := -\tau^2(B^n)^2\int_0^1 (1-s)\mathrm{e}^{-is\tau B^n}u(t_n)\,ds.$$

It follows that the truncation error of the Lie-Trotter splitting scheme (3.1) can be written as

$$\begin{aligned}
\xi^n &= \mathrm{e}^{-i\tau\Gamma}\left(i\tau B^n u(t_n) - i\int_0^\tau \mathrm{e}^{is\Gamma}B^n(s)u(t_n+s)\,ds + \xi_1^n\right)\\
&= \mathrm{e}^{-i\tau\Gamma}\left(i\int_0^\tau \big(G^n(0) - G^n(s)\big)\,ds + \xi_1^n\right)\\
&= \mathrm{e}^{-i\tau\Gamma}\left(-i\int_0^\tau\int_0^s \partial_w G^n(w)\,dw\,ds + \xi_1^n\right),
\end{aligned}$$

where $G^n(w) := \mathrm{e}^{iw\Gamma}B^n(w)u(t_n+w)$. Since $\Gamma = \mathcal{O}(1/\varepsilon)$, assumptions (A) and (B) give

$$\xi_1^n = \mathcal{O}\left(\tau^2\right), \quad \partial_w G^n(w) = \mathcal{O}\left(\frac{1}{\varepsilon}\right) \quad \text{for all} \quad w \in [0,\tau].$$

It follows that $\xi^n = \mathcal{O}(\tau^2/\varepsilon)$. This implies the first-order accuracy of the Lie-Trotter splitting scheme (3.1) with the meshing strategy $\tau \le C\varepsilon$.

### 3.2. Strang splitting

The local truncation error of the Strang splitting scheme (3.2) is defined as

$$\xi^n := u(t_{n+1}) - \Psi_{\tau/2}^{\mathrm{k}} \circ \Psi_\tau^{\mathrm{p}} \circ \Psi_{\tau/2}^{\mathrm{k}}\big(u(t_n)\big).$$

Substituting (3.3) into (3.4), we write $u(t_{n+1})$ as

$$\begin{aligned}
u(t_{n+1}) = \mathrm{e}^{-i\tau\Gamma}u(t_n) &- i\int_0^\tau \mathrm{e}^{-i(\tau-s)\Gamma}B^n(s)\mathrm{e}^{-is\Gamma}u(t_n)\,ds\\
&- \int_0^\tau\int_0^s \mathrm{e}^{-i(\tau-s)\Gamma}B^n(s)\mathrm{e}^{-i(s-w)\Gamma}B^n(w)u(t_n+w)\,dw\,ds.
\end{aligned} \tag{3.5}$$

Besides, the term $\Psi^{\mathrm{k}}_{\tau/2}\circ\Psi^{\mathrm{p}}_{\tau}\circ\Psi^{\mathrm{k}}_{\tau/2}(u(t_n))$ can be written as

$$\Psi^{\mathrm{k}}_{\tau/2}\circ\Psi^{\mathrm{p}}_{\tau}\circ\Psi^{\mathrm{k}}_{\tau/2}\big(u(t_n)\big)=\mathrm{e}^{-i\tau\Gamma/2}\mathrm{e}^{-i\tau\widetilde{B}^n}\mathrm{e}^{-i\tau\Gamma/2}u(t_n),$$

where

$$\widetilde{B}^n=V\cdot Id+\lambda\Big(\big(\mathrm{e}^{-i\tau\Gamma/2}u(t_n)\big)^*\beta\mathrm{e}^{-i\tau\Gamma/2}u(t_n)\Big)\beta.$$

Using the Taylor's expansion of

$$\mathrm{e}^{-i\tau\widetilde{B}^n}=Id-i\tau\widetilde{B}^n-\tau^2(\widetilde{B}^n)^2\int_0^1(1-s)\mathrm{e}^{-is\tau\widetilde{B}^n}\,ds,$$

we have

$$\begin{aligned}&\Psi^{\mathrm{k}}_{\tau/2}\circ\Psi^{\mathrm{p}}_{\tau}\circ\Psi^{\mathrm{k}}_{\tau/2}\big(u(t_n)\big)\\&=\mathrm{e}^{-i\tau\Gamma}u(t_n)-i\tau\mathrm{e}^{-i\tau\Gamma/2}\widetilde{B}^n\mathrm{e}^{-i\tau\Gamma/2}u(t_n)\\&\quad-\tau^2\mathrm{e}^{-i\tau\Gamma/2}(\widetilde{B}^n)^2\int_0^1(1-s)\mathrm{e}^{-is\tau\widetilde{B}^n}\mathrm{e}^{-i\tau\Gamma/2}u(t_n)\,ds.\end{aligned}$$

Subtracting it from (3.5), we write the local truncation of the Strang splitting scheme (3.2) as

$$\xi^n=\left(i\tau G_1^n\Big(\frac{\tau}{2}\Big)-i\int_0^\tau G_1^n(s)\,ds\right)+\left(\frac{\tau^2}{2}G_2^n\Big(\frac{\tau}{2},\frac{\tau}{2}\Big)-\int_0^\tau\int_0^s G_2^n(s,w)\,dwds\right)+\eta_1^n+\eta_2^n+\eta_3^n$$

with

$$\begin{aligned}&G_1^n(s):=\mathrm{e}^{-i(\tau-s)\Gamma}B^n(s)\mathrm{e}^{-is\Gamma}u(t_n),\\&G_2^n(s,w):=\mathrm{e}^{-i(\tau-s)\Gamma}B^n(s)\mathrm{e}^{-i(s-w)\Gamma}B^n(w)\mathrm{e}^{-iw\Gamma}u(t_n),\\&\eta_1^n:=i\tau\left(\mathrm{e}^{-i\tau\Gamma/2}\widetilde{B}^n\mathrm{e}^{-i\tau\Gamma/2}u(t_n)-G_1^n\Big(\frac{\tau}{2}\Big)\right),\\&\eta_2^n:=\int_0^\tau\int_0^s\Big(G_2^n(s,w)-\mathrm{e}^{-i(\tau-s)\Gamma}B^n(s)\mathrm{e}^{-i(s-w)\Gamma}B^n(w)u(t_n+w)\Big)\,dwds,\\&\eta_3^n:=\tau^2\left(\mathrm{e}^{-i\tau\Gamma/2}(\widetilde{B}^n)^2\int_0^1(1-s)\mathrm{e}^{-is\tau\widetilde{B}^n}\mathrm{e}^{-i\tau\Gamma/2}u(t_n)\,ds-\frac{1}{2}G_2^n\Big(\frac{\tau}{2},\frac{\tau}{2}\Big)\right).\end{aligned}$$

Next, we estimate the expression $\xi^n$ term by term under assumptions (A) and (B). According to the quadrature rules and the Taylor's expansion, we have

$$\begin{aligned}&i\tau G_1^n\Big(\frac{\tau}{2}\Big)-i\int_0^\tau G_1^n(s)\,ds=-i\int_0^\tau\int_0^s(s-w)\partial_w^2G_1^n(w)\,dwds=\mathscr{O}\left(\frac{\tau^3}{\varepsilon^2}\right),\\&\frac{\tau^2}{2}G_2^n\Big(\frac{\tau}{2},\frac{\tau}{2}\Big)-\int_0^\tau\int_0^s G_2^n(s,w)\,dwds\\&=\int_0^\tau\int_0^s\left(\int_s^{\tau/2}\partial_{\sigma_1}G_2^n\Big(\sigma_1,\frac{\tau}{2}\Big)\,d\sigma_1+\int_w^{\tau/2}\partial_{\sigma_2}G_2^n(s,\sigma_2)\,d\sigma_2\right)dwds=\mathscr{O}\left(\frac{\tau^3}{\varepsilon}\right).\end{aligned}$$

Recalling the Eq. (3.3) gives

$$\eta_2^n = -\int_0^\tau \int_0^s \int_0^w \mathrm{e}^{-i(\tau-s)\Gamma} B^n(s) \mathrm{e}^{-i(s-w)\Gamma} B^n(w) \mathrm{e}^{-i(w-\sigma)\Gamma} B^n(\sigma) u(t_n+\sigma)\, d\sigma dw ds = \mathscr{O}\left(\tau^3\right).$$

In order to estimate $\eta_1^n$ and $\eta_3^n$, we first measure the difference between $u(t_n+\tau/2)$ and $\mathrm{e}^{-i\tau\Gamma/2}u(t_n)$. Employing (3.3) and Taylor's expansion again gives

$$\begin{aligned} u\left(t_n+\frac{\tau}{2}\right) &= \mathrm{e}^{-i\tau\Gamma/2}u(t_n) - i\int_0^{\tau/2} \mathrm{e}^{-i(\tau/2-w)\Gamma} B^n(w) u(t_n+w)\, dw \\ &= \mathrm{e}^{-i\tau\Gamma/2}u(t_n) - i\frac{\tau}{2}\mathrm{e}^{-i\tau\Gamma/2} B^n u(t_n) + \mathscr{O}\left(\frac{\tau^2}{\varepsilon}\right). \end{aligned}$$

Since $B^n$ and $\beta$ are real and diagonal, we have

$$\left(u(t_n)\right)^* \beta\left(iB^n u(t_n)\right) + \left(iB^n u(t_n)\right)^* \beta u(t_n) = 0.$$

In addition, by diagonalizing $\Gamma$ we show the relation

$$\left(\mathrm{e}^{-i\tau\Gamma/2}u(t_n)\right)^* \beta\left(i\mathrm{e}^{-i\tau\Gamma/2} B^n u(t_n)\right) + \left(i\mathrm{e}^{-i\tau\Gamma/2} B^n u(t_n)\right)^* \beta \mathrm{e}^{-i\tau\Gamma/2} u(t_n) = 0.$$

Thus,

$$\left(u\left(t_n+\frac{\tau}{2}\right)\right)^* \beta u\left(t_n+\frac{\tau}{2}\right) - \left(\mathrm{e}^{-i\tau\Gamma/2}u(t_n)\right)^* \beta \mathrm{e}^{-i\tau\Gamma/2} u(t_n) = \mathscr{O}\left(\frac{\tau^2}{\varepsilon}\right),$$

which implies $\widetilde{B}^n - B^n(\tau/2) = \mathscr{O}(\tau^2/\varepsilon)$. Consequently, we get

$$\begin{aligned} \eta_1^n &= \tau \mathrm{e}^{-i\tau\Gamma/2}\left(\widetilde{B}^n - B^n\left(\frac{\tau}{2}\right)\right)\mathrm{e}^{-i\tau\Gamma/2}u(t_n) = \mathscr{O}\left(\frac{\tau^3}{\varepsilon}\right), \\ \eta_3^n &= \tau^2 \mathrm{e}^{-i\tau\Gamma/2}\left((\widetilde{B}^n)^2 \int_0^1 (1-s)\mathrm{e}^{-is\tau\widetilde{B}^n} ds - \frac{1}{2}\left(B^n\left(\frac{\tau}{2}\right)\right)^2\right)\mathrm{e}^{-i\tau\Gamma/2}u(t_n) \\ &= \mathscr{O}\left(\tau^3\right) + \mathscr{O}\left(\frac{\tau^4}{\varepsilon}\right). \end{aligned}$$

Therefore, the local truncation error of the Strang splitting scheme (3.2) is $\xi^n = \mathscr{O}(\tau^3/\varepsilon^2)$, and it is second-order accurate with the meshing strategy $\tau \le C\varepsilon$.

## 4. Exponential Integrators

In this section, we consider the exponential integrators [29] for solving the NDE (1.1), which are constructed based on the integral form of the solution

$$u(t_{n+1}) = \mathrm{e}^{-i\tau\Gamma}u(t_n) - i\int_0^\tau \mathrm{e}^{-i(\tau-s)\Gamma} H\big(u(t_n+s)\big) ds, \quad n \ge 0 \tag{4.1}$$

with $H(u) := Vu + \lambda(u^*\beta u)\beta u$. Approximating $H(u(t_n+s))$ by $H(u(t_n))$ and $H(u(t_n)) + (s/\tau)(H(u(t_n)) - H(u(t_{n-1})))$ respectively result in the first-order exponential integrator (EI1)

$$u^{n+1} = \mathrm{e}^{-i\tau\Gamma}u^n - i\tau\varphi_1(-i\tau\Gamma)H(u^n), \quad n \geq 0,$$

and the second-order exponential integrator (EI2)

$$\begin{aligned} u^1 &= \mathrm{e}^{-i\tau\Gamma}u^0 - i\tau\varphi_1(-i\tau\Gamma)H(u^0), \\ u^{n+1} &= \mathrm{e}^{-i\tau\Gamma}u^n - i\tau\varphi_1(-i\tau\Gamma)H(u^n) - i\tau\varphi_2(-i\tau\Gamma)\big(H(u^n) - H(u^{n-1})\big), \quad n \geq 1 \end{aligned}$$

with

$$\varphi_1(z) = \frac{\mathrm{e}^z - 1}{z}, \quad \varphi_2(z) = \frac{\mathrm{e}^z - z - 1}{z^2}. \tag{4.2}$$

Therefore, the corresponding truncation errors are

$$\begin{aligned} \xi^n_{\mathrm{EI1}} &:= u(t_{n+1}) - \mathrm{e}^{-i\tau\Gamma}u(t_n) - i\tau\varphi_1(-i\tau\Gamma)H\big(u(t_n)\big) \\ &= -i\int_0^\tau \mathrm{e}^{-i(\tau-s)\Gamma}\Big[H\big(u(t_n+s)\big) - H\big(u(t_n)\big)\Big]ds \\ &= -i\int_0^\tau\int_0^s \mathrm{e}^{-i(\tau-s)\Gamma}\partial_w H\big(u(t_n+w)\big)\,dwds, \\ \xi^n_{\mathrm{EI2}} &:= u(t_{n+1}) - \mathrm{e}^{-i\tau\Gamma}u(t_n) - i\tau\varphi_1(-i\tau\Gamma)H\big(u(t_n)\big) \\ &\quad - i\tau\varphi_2(-i\tau\Gamma)\Big(H\big(u(t_n)\big) - H\big(u(t_{n-1})\big)\Big) \\ &= -i\int_0^\tau \mathrm{e}^{-i(\tau-s)\Gamma}\left(H\big(u(t_n+s)\big) - H\big(u(t_n)\big) - \frac{s}{\tau}\Big(H\big(u(t_n)\big) - H\big(u(t_{n-1})\big)\Big)\right)ds \\ &= -\frac{i}{\tau}\int_0^\tau \mathrm{e}^{-i(\tau-s)\Gamma}\int_0^s\int_{-\tau}^0\int_\rho^\sigma \partial_w^2 H\big(u(t_n+w)\big)\,dwd\rho d\sigma ds. \end{aligned}$$

According to assumptions (A) and (B), it can be seen that

$$\partial_w H\big(u(t_n+w)\big) = \mathscr{O}\left(\frac{1}{\varepsilon}\right), \quad \partial_w^2 H\big(u(t_n+w)\big) = \mathscr{O}\left(\frac{1}{\varepsilon^2}\right) \quad \text{for all} \quad w \in [0,\tau],$$

which implies that $\xi_{\mathrm{EI1}} = \mathscr{O}(\tau^2/\varepsilon)$, $\xi_{\mathrm{EI2}} = \mathscr{O}(\tau^3/\varepsilon^2)$. Therefore, EI1 and EI2 can reach their optimal convergence rates only when the meshing strategy is $\tau \leq C\varepsilon$.

## 5. Uniformly Accurate Methods

It can be seen that the above classical methods all need to impose restrictions on the time-step size to achieve optimal convergence accuracies. This causes inconvenience and inefficiency in practical computing. Therefore, in this section we present a uniformly accurate method for solving the NDE (1.1) in the massless nonrelativistic regime, without restrictions on the time-step size for all $\varepsilon \in (0,1]$.

As already mentioned, in order to design a UA method, one needs to utilize a certain technique to explicitly filter out the dominant highly oscillatory phases and deal with them exactly. The technique we use here is still operator splitting, but it is different from that in [15,16]. In [15,16], the authors solve the Dirac equation and an NDE in the nonrelativistic regime — i.e. the Eq. (1.1) with $\delta = 1/\varepsilon^2$. In the nonrelativistic regime, the mass term — i.e. $\delta\beta u(t,x)$, is an $\mathscr{O}(1/\varepsilon^2)$ term and it has to be treated explicitly and exactly. Therefore, when writing the equation in an integral form with Duhamel's principle, the mass term has to be involved in the linear part as in (4.1). Otherwise, it appears in the integration and causes a large error after approximation.

However, things have changed in our case. In the massless and nonrelativistic regime, the mass term becomes $\mathscr{O}(1)$, so that $-i\alpha\partial_x u(t,x)/\varepsilon$ can be treated linearly. Therefore, we apply the Duhamel's principle for the NDE (1.1) by dropping the mass term into the integration as

$$u(t_n+s) = \mathrm{e}^{-s\alpha\partial_x/\varepsilon}u(t_n) - i\int_0^s \mathrm{e}^{-(s-w)\alpha\partial_x/\varepsilon}\Big[\delta\beta u(t_n+w) + Vu(t_n+w) + F\big(u(t_n+w)\big)\Big]dw. \tag{5.1}$$

The advantage of this integral form is that the linear operator $\alpha\partial_x$ and the evolution operator $\mathrm{e}^{(s-w)\alpha\partial_x/\varepsilon}$ can be perfectly diagonalized similar to (1.2)-(1.3). It can be seen from (1.3) that we can explicitly extract the highly oscillatory phases $\pm\mathrm{e}^{s\partial_x/\varepsilon}$ from the evolution operator. Thus, the integral can be calculated exactly after applying the nested Picard iteration, resulting in a UA scheme. The detailed derivation based on assumptions (A) and (B), is presented below.

## 5.1. A uniformly accurate scheme

The UA scheme is constructed based on the integral equation (5.1) and the nested Picard iteration. More exactly, we take a robust approximate of $u(t_n+w)$ by dropping the integral term of (5.1), i.e.

$$u^{n,0}(w) := \mathrm{e}^{-w\alpha\partial_x/\varepsilon}u(t_n), \quad 0 \le w \le s \le \tau. \tag{5.2}$$

Replace $u(t_n+w)$ in (5.1) by $u^{n,0}(w)$, and obtain a refined approximation of $u(t_n+s)$, viz.

$$u^{n,1}(s) := \mathrm{e}^{-s\alpha\partial_x/\varepsilon}u(t_n) - i\int_0^s \mathrm{e}^{-(s-w)\alpha\partial_x/\varepsilon}\Big[\delta\beta u^{n,0}(w) + Vu^{n,0}(w) + F\left(u^{n,0}(w)\right)\Big]dw. \tag{5.3}$$

Calculating the above integral exactly, we could obtain a first-order UA scheme. Define

$$\begin{aligned} I_1(t_n,s) &:= \delta\int_0^s \mathrm{e}^{w\alpha\partial_x/\varepsilon}\beta u^{n,0}(w)\,dw = \delta\int_0^s \mathrm{e}^{w\alpha\partial_x/\varepsilon}\beta\mathrm{e}^{-w\alpha\partial_x/\varepsilon}u(t_n)dw, \\ I_2(t_n,s) &:= \int_0^s \mathrm{e}^{w\alpha\partial_x/\varepsilon}Vu^{n,0}(w)\,dw = \int_0^s \mathrm{e}^{w\alpha\partial_x/\varepsilon}V\mathrm{e}^{-w\alpha\partial_x/\varepsilon}u(t_n)dw, \\ I_3(t_n,s) &:= \int_0^s \mathrm{e}^{w\alpha\partial_x/\varepsilon}F(u^{n,0}(w))\,dw = \int_0^s \mathrm{e}^{w\alpha\partial_x/\varepsilon}F\left(\mathrm{e}^{-w\alpha\partial_x/\varepsilon}u(t_n)\right)dw. \end{aligned} \tag{5.4}$$

Since the operators in the integrand are not commutative, these integrals are not easy to calculate. However, they can be exactly integrated by employing an operator splitting. Thus taking into account (1.3) and using the identities $\Pi_\pm\beta\Pi_\pm = \mathbf{0}$, $\Pi_\pm\beta\Pi_\mp = \beta\Pi_\mp$, we rewrite the integrand of $I_1(t_n,s)$ as

$$\begin{aligned}
&\mathrm{e}^{w\alpha\partial_x/\varepsilon}\beta\mathrm{e}^{-w\alpha\partial_x/\varepsilon}u(t_n)\\
&=\left(\mathrm{e}^{w\partial_x/\varepsilon}\Pi_+ + \mathrm{e}^{-w\partial_x/\varepsilon}\Pi_-\right)\beta\left(\mathrm{e}^{-w\partial_x/\varepsilon}\Pi_+ + \mathrm{e}^{w\partial_x/\varepsilon}\Pi_-\right)u(t_n)\\
&=\left(\mathrm{e}^{2w\partial_x/\varepsilon}\beta\Pi_- + \mathrm{e}^{-2w\partial_x/\varepsilon}\beta\Pi_+\right)u(t_n).
\end{aligned}$$

Integrating the resulting expression gives

$$I_1(t_n,s) = s\delta\left[\varphi_1\left(\frac{2s}{\varepsilon}\partial_x\right)\beta\Pi_- + \varphi_1\left(-\frac{2s}{\varepsilon}\partial_x\right)\beta\Pi_+\right]u(t_n), \tag{5.5}$$

where $\varphi_1(\cdot)$ is defined in (4.2).

Similarly, we write the integrand of $I_2(t_n)$ as

$$\begin{aligned}
&\mathrm{e}^{w\alpha\partial_x/\varepsilon}V\mathrm{e}^{-w\alpha\partial_x/\varepsilon}u(t_n)\\
&=\left(\mathrm{e}^{w\partial_x/\varepsilon}\Pi_+ + \mathrm{e}^{-w\partial_x/\varepsilon}\Pi_-\right)V\left(\mathrm{e}^{-w\partial_x/\varepsilon}\Pi_+ + \mathrm{e}^{w\partial_x/\varepsilon}\Pi_-\right)u(t_n)\\
&=\left(\mathrm{e}^{w\partial_x/\varepsilon}V\mathrm{e}^{-w\partial_x/\varepsilon}\Pi_+ + \mathrm{e}^{-w\partial_x/\varepsilon}V\mathrm{e}^{w\partial_x/\varepsilon}\Pi_-\right)u(t_n)
\end{aligned}$$

with $\Pi_\pm\Pi_\mp = \mathbf{0}, \Pi_\pm\Pi_\pm = \Pi_\pm$. Unlike $I_1(t_n)$, we cannot take exact integration for the above integrand since $\mathrm{e}^{\pm w\partial_x/\varepsilon}$ does not commute with $V$. Inspired by the idea in [36, 38], we analyze it in the Fourier space — i.e.

$$\begin{aligned}
&\mathrm{e}^{w\partial_x/\varepsilon}V\mathrm{e}^{-w\partial_x/\varepsilon}\Pi_+u(t_n)\\
&=\sum_{l\in\mathbb{Z}}\sum_{\substack{l_1,l_2\in\mathbb{Z}\\ l_1+l_2=l}}\mathrm{e}^{ilx}\mathrm{e}^{ilw/\varepsilon}\widehat{V}_{l_1}\mathrm{e}^{-il_2w/\varepsilon}\Pi_+\widehat{u}_{l_2}\\
&=\sum_{l\in\mathbb{Z}}\sum_{\substack{l_1,l_2\in\mathbb{Z}\\ l_1+l_2=l}}\mathrm{e}^{ilx}\mathrm{e}^{i(l-l_2)w/\varepsilon}\widehat{V}_{l_1}\Pi_+\widehat{u}_{l_2}\\
&=(\mathrm{e}^{w\partial_x/\varepsilon}V)\Pi_+u(t_n),\\
&\mathrm{e}^{-w\partial_x/\varepsilon}V\mathrm{e}^{w\partial_x/\varepsilon}\Pi_-u(t_n) = (\mathrm{e}^{-w\partial_x/\varepsilon}V)\Pi_-u(t_n).
\end{aligned}$$

Integrating the resulting expression yields

$$I_2(t_n,s) = s\left[\left(\varphi_1\left(\frac{s}{\varepsilon}\partial_x\right)V\right)\Pi_+ + \left(\varphi_1\left(-\frac{s}{\varepsilon}\partial_x\right)V\right)\Pi_-\right]u(t_n). \tag{5.6}$$

Considering $I_3(t_n,s)$, we first write

$$\begin{aligned}
f(t_n) :&= \left(\mathrm{e}^{-w\alpha\partial_x/\varepsilon}u(t_n)\right)^*\beta\left(\mathrm{e}^{-w\alpha\partial_x/\varepsilon}u(t_n)\right)\\
&=\left[\left(\mathrm{e}^{w\partial_x/\varepsilon}u(t_n)\right)^*\mathrm{e}^{w\partial_x/\varepsilon}\beta\Pi_- + \left(\mathrm{e}^{w\partial_x/\varepsilon}u(t_n)\right)^*\mathrm{e}^{-w\partial_x/\varepsilon}\beta\Pi_+\right]u(t_n)\\
&=\frac{1}{2}\Big[\left(\mathrm{e}^{w\partial_x/\varepsilon}u_-(t_n)\right)\left(\mathrm{e}^{-w\partial_x/\varepsilon}\overline{u_+}(t_n)\right) + \left(\mathrm{e}^{w\partial_x/\varepsilon}\overline{u_-}(t_n)\right)\left(\mathrm{e}^{-w\partial_x/\varepsilon}u_+(t_n)\right)\Big]
\end{aligned}$$

with

$$u_{\pm}(t_n) := u_1(t_n) \pm u_2(t_n), \quad u(t_n) = \big(u_1(t_n), u_2(t_n)\big)^T.$$

Now the integrand in $I_3(t_n)$ takes the form

$$\begin{aligned}
&\mathrm{e}^{w\alpha\partial_x/\varepsilon} F\left(\mathrm{e}^{-w\alpha\partial_x/\varepsilon} u(t_n)\right) \\
&= \lambda \mathrm{e}^{w\alpha\partial_x/\varepsilon} f(t_n) \beta \mathrm{e}^{-w\alpha\partial_x/\varepsilon} u(t_n) \\
&= \lambda \left(\mathrm{e}^{w\partial_x/\varepsilon}\Pi_+ + \mathrm{e}^{-w\partial_x/\varepsilon}\Pi_-\right) f(t_n) \beta \left(\mathrm{e}^{-w\partial_x/\varepsilon}\Pi_+ + \mathrm{e}^{w\partial_x/\varepsilon}\Pi_-\right) u(t_n) \\
&= \lambda \Big[\mathrm{e}^{w\partial_x/\varepsilon} f(t_n) \mathrm{e}^{w\partial_x/\varepsilon} \beta \Pi_- + \mathrm{e}^{-w\partial_x/\varepsilon} f(t_n) \mathrm{e}^{-w\partial_x/\varepsilon} \beta \Pi_+\Big] u(t_n) \\
&= \frac{\lambda}{2}\left[\mathrm{e}^{w\partial_x/\varepsilon} f(t_n) \mathrm{e}^{w\partial_x/\varepsilon} u_-(t_n) \begin{pmatrix} 1 \\ 1 \end{pmatrix} + \mathrm{e}^{-w\partial_x/\varepsilon} f(t_n) \mathrm{e}^{-w\partial_x/\varepsilon} u_+(t_n) \begin{pmatrix} 1 \\ -1 \end{pmatrix}\right].
\end{aligned}$$

Consider each term in the Fourier space again, we obtain

$$\begin{aligned}
&\mathrm{e}^{w\partial_x/\varepsilon}\Big[\big(\mathrm{e}^{w\partial_x/\varepsilon} u_-(t_n)\big)\big(\mathrm{e}^{-w\partial_x/\varepsilon}\overline{u_+}(t_n)\big)\mathrm{e}^{w\partial_x/\varepsilon} u_-(t_n)\Big] \\
&= \sum_{l\in\mathbb{Z}} \sum_{\substack{l_1,l_2,l_3\in\mathbb{Z} \\ l_1+l_2+l_3=l}} \mathrm{e}^{ilx} \mathrm{e}^{ilw/\varepsilon} \mathrm{e}^{il_1 w/\varepsilon} \widehat{\big(u_-(t_n)\big)}_{l_1} \mathrm{e}^{-il_2 w/\varepsilon} \widehat{\big(\overline{u_+}(t_n)\big)}_{l_2} \mathrm{e}^{il_3 w/\varepsilon} \widehat{\big(u_-(t_n)\big)}_{l_3} \\
&= \sum_{l\in\mathbb{Z}} \sum_{\substack{l_1,l_2,l_3\in\mathbb{Z} \\ l_1+l_2+l_3=l}} \mathrm{e}^{ilx} \mathrm{e}^{2i(l_1+l_3)w/\varepsilon} \widehat{\big(u_-(t_n)\big)}_{l_1} \widehat{\big(\overline{u_+}(t_n)\big)}_{l_2} \widehat{\big(u_-(t_n)\big)}_{l_3} \\
&= \Big(\mathrm{e}^{2w\partial_x/\varepsilon}\big(u_-(t_n)\big)^2\Big)\overline{u_+}(t_n),
\end{aligned}$$

$$\begin{aligned}
&\mathrm{e}^{w\partial_x/\varepsilon}\Big[\big(\mathrm{e}^{w\partial_x/\varepsilon}\overline{u_-}(t_n)\big)\big(\mathrm{e}^{-w\partial_x/\varepsilon} u_+(t_n)\big)\mathrm{e}^{w\partial_x/\varepsilon} u_-(t_n)\Big] \\
&= \big(\mathrm{e}^{2w\partial_x/\varepsilon}|u_-(t_n)|^2\big) u_+(t_n),
\end{aligned}$$

$$\begin{aligned}
&\mathrm{e}^{-w\partial_x/\varepsilon}\Big[\big(\mathrm{e}^{w\partial_x/\varepsilon} u_-(t_n)\big)\big(\mathrm{e}^{-w\partial_x/\varepsilon}\overline{u_+}(t_n)\big)\mathrm{e}^{-w\partial_x/\varepsilon} u_+(t_n)\Big] \\
&= \big(\mathrm{e}^{-2w\partial_x/\varepsilon}|u_+(t_n)|^2\big) u_-(t_n),
\end{aligned}$$

$$\begin{aligned}
&\mathrm{e}^{-w\partial_x/\varepsilon}\Big[\big(\mathrm{e}^{w\partial_x/\varepsilon}\overline{u_-}(t_n)\big)\big(\mathrm{e}^{-w\partial_x/\varepsilon} u_+(t_n)\big)\mathrm{e}^{-w\partial_x/\varepsilon} u_+(t_n)\Big] \\
&= \Big(\mathrm{e}^{-2w\partial_x/\varepsilon}\big(u_+(t_n)\big)^2\Big)\overline{u_-}(t_n).
\end{aligned}$$

Hence, we have

$$\begin{aligned}
I_3(t_n,s) = &\frac{s\lambda}{4}\left[\overline{u_+}(t_n)\varphi_1\left(\frac{2s}{\varepsilon}\partial_x\right)\big(u_-(t_n)\big)^2 + u_+(t_n)\varphi_1\left(\frac{2s}{\varepsilon}\partial_x\right)|u_-(t_n)|^2\right]\begin{pmatrix} 1 \\ 1 \end{pmatrix} \\
&+ \frac{s\lambda}{4}\left[\overline{u_-}(t_n)\varphi_1\left(-\frac{2s}{\varepsilon}\partial_x\right)\big(u_+(t_n)\big)^2 + u_-(t_n)\varphi_1\left(-\frac{2s}{\varepsilon}\partial_x\right)|u_+(t_n)|^2\right]\begin{pmatrix} 1 \\ -1 \end{pmatrix}.
\end{aligned} \tag{5.7}$$

Taking into account (5.3), (5.5)-(5.7), we can consider the following uniformly accurate scheme for the NDE (1.1):

$$u^{n+1} = \mathrm{e}^{-\tau\alpha\partial_x/\varepsilon} u^n - i\mathrm{e}^{-\tau\alpha\partial_x/\varepsilon}\left(I_1^n + I_2^n + I_3^n\right) =: \Phi_{\mathrm{ext}}(u^n), \quad n \geq 0, \tag{5.8}$$

where

$$
\begin{aligned}
I_1^n &:= \tau\delta\left[\varphi_1\left(\frac{2\tau}{\varepsilon}\partial_x\right)\beta\Pi_- + \varphi_1\left(-\frac{2\tau}{\varepsilon}\partial_x\right)\beta\Pi_+\right]u^n,\\
I_2^n &:= \tau\left[\left(\varphi_1\left(\frac{\tau}{\varepsilon}\partial_x\right)V\right)\Pi_+ + \left(\varphi_1\left(-\frac{\tau}{\varepsilon}\partial_x\right)V\right)\Pi_-\right]u^n,\\
I_3^n &:= \frac{\tau\lambda}{4}\left(\overline{u_+^n}\varphi_1\left(\frac{2\tau}{\varepsilon}\partial_x\right)\left(u_-^n\right)^2 + u_+^n\varphi_1\left(\frac{2\tau}{\varepsilon}\partial_x\right)|u_-^n|^2\right)\begin{pmatrix}1\\1\end{pmatrix}\\
&\quad + \frac{\tau\lambda}{4}\left(u_-^n\varphi_1\left(-\frac{2\tau}{\varepsilon}\partial_x\right)\left|u_+^n\right|^2 + \overline{u_-^n}\varphi_1\left(-\frac{2\tau}{\varepsilon}\partial_x\right)\left(u_+^n\right)^2\right)\begin{pmatrix}1\\-1\end{pmatrix}
\end{aligned}
\tag{5.9}
$$

with $u^n = (u_1^n, u_2^n)^T$, $u_\pm^n = u_1^n \pm u_2^n$.

It can be seen that the UA scheme can be explicitly expressed in the physical space, and it can be easily implemented by a Fourier pseudospectral method. We could establish the error bound for the above UA scheme as follows.

**Theorem 5.1** (Convergence of UA ). *Let $u^n$ be the numerical solution of the UA scheme* (5.8)-(5.9) *for the NDE* (1.1). *Let $r > 1/2$ and $u \in L^\infty([0,T];(H^r)^2)$ for some $T > 0$. Then there exist constants $\tau_0, C > 0$ depending on $\|u\|_{L^\infty([0,T];(H^r)^2)}$ and $T$, such that for all $0 < \tau \le \tau_0$ and $0 \le t_n \le T$, we have the following error estimate for the UA scheme* (5.8)*:*

$$\|u(t_n) - u^n\|_r \le C\tau,$$

*where $\|u\|_r = \sqrt{\|u_1\|_{H^r}^2 + \|u_2\|_{H^r}^2}$, $u = (u_1,u_2)^T \in (H^r(\mathbb{T}))^2$, and $\|\cdot\|_{H^r} = \|\cdot\|_{H^r(\mathbb{T})}$ is the standard Sobolev norm.*

*Proof.* Denote $e^n := u(t_n) - u^n$. The triangle inequality gives

$$\|e^{n+1}\|_r \le \|u(t_{n+1}) - \Phi_{\text{ext}}(u(t_n))\|_r + \|\Phi_{\text{ext}}(u(t_n)) - \Phi_{\text{ext}}(u^n)\|_r. \tag{5.10}$$

We first analyze the local truncation error

$$\xi^n := u(t_{n+1}) - \Phi_{\text{ext}}\big(u(t_n)\big)$$

of the UA scheme (5.8) at $t_n$, $n \ge 0$.

The derivation of the UA scheme implies that $\Phi_{\text{ext}}(u(t_n)) = u^{n,1}(\tau)$, since $I_1(t_n,s)$, $I_2(t_n,s)$ and $I_3(t_n,s)$ in (5.4) are all exactly calculated. Thus subtracting (5.3) from (5.1) and taking $s = \tau$, we obtain

$$
\begin{aligned}
\xi^n = -i\int_0^\tau \mathrm{e}^{-(\tau-w)\alpha\partial_x/\varepsilon}\Big[&\delta\beta\left(u(t_n+w) - u^{n,0}(w)\right) + V\left(u(t_n+w) - u^{n,0}(w)\right)\\
&+ F\big(u(t_n+w)\big) - F\left(u^{n,0}(w)\right)\Big]dw.
\end{aligned}
$$

The Eqs. (1.2) and (1.3) give

$$\left|\widehat{\left(\mathrm{e}^{s\alpha\partial_x/\varepsilon}\Phi\right)}_l\right|^2 = \left|\left(\mathrm{e}^{isl/\varepsilon}\Pi_+ + \mathrm{e}^{-isl/\varepsilon}\Pi_-\right)\widehat{\Phi}_l\right|^2 = \left|\widehat{\Phi}_l\right|^2, \quad l \in \mathbb{Z}, \quad s \in \mathbb{R}$$

for a general function $\Phi(x):\mathbb{T}\to\mathbb{C}^2$, i.e. $e^{s\alpha\partial_x/\varepsilon}$ is isometric in $H^r$ space. Under assumptions (A) and (B), and thanks to the triangle inequality and bilinear estimates since $r>1/2$, we have

$$\begin{aligned}\|\xi^n\|_r &\le |\delta|\int_0^\tau \left\|u(t_n+w)-u^{n,0}(w)\right\|_r dw\\ &\quad+\int_0^\tau \left\|V\big(u(t_n+w)-u^{n,0}(w)\big)\right\|_r dw\\ &\quad+\int_0^\tau \left\|F\big(u(t_n+w)\big)-F\left(u^{n,0}(w)\right)\right\|_r dw\\ &\le C\int_0^\tau \left\|u(t_n+w)-u^{n,0}(w)\right\|_r dw.\end{aligned}$$

Recalling (5.1) and (5.2), we have

$$\begin{aligned}&\left\|u(t_n+w)-u^{n,0}(w)\right\|_r\\ &\le\int_0^w \left[\|\delta\beta u(t_n+\sigma)\|_r+\|Vu(t_n+\sigma)\|_r+\|F\left(u(t_n+\sigma)\right)\|_r\right]d\sigma\\ &\le C\int_0^w \|u(t_n+\sigma)\|_r d\sigma\le C\tau\|u\|_{L^\infty([0,T];(H^r)^2)},\quad \forall 0\le w\le\tau.\end{aligned}$$

It follows that

$$\|\xi^n\|_r\le C\tau^2. \tag{5.11}$$

Consider the other local truncation error — viz.

$$\eta^n:=\Phi_{\text{ext}}\big(u(t_n)\big)-\Phi_{\text{ext}}(u^n),\quad n\ge 0.$$

Recalling the UA scheme (5.8), we write

$$\eta^n=e^{-\tau\alpha\partial_x/\varepsilon}e^n-ie^{-\tau\alpha\partial_x/\varepsilon}\left[I_1(t_n,\tau)-I_1^n+I_2(t_n,\tau)-I_2^n+I_3(t_n,\tau)-I_3^n\right],$$

where $I_k(t_n,\tau), k=1,2,3$ are defined in (5.5)-(5.7). Since $e^{-\tau\alpha\partial_x/\varepsilon}$ is isometric, we have

$$\|\eta^n\|_r\le\|e^n\|_r+\left\|I_1(t_n,\tau)-I_1^n\right\|_r+\left\|I_2(t_n,\tau)-I_2^n\right\|_r+\left\|I_3(t_n,\tau)-I_3^n\right\|_r,\quad n\ge 0. \tag{5.12}$$

Subtracting $I_1^n$ in (5.9) from $I_1(t_n,\tau)$ in (5.5) gives

$$\left\|I_1(t_n,\tau)-I_1^n\right\|_r=\tau\delta\left\|\left[\varphi_1\left(\frac{2\tau}{\varepsilon}\partial_x\right)\beta\Pi_-+\varphi_1\left(-\frac{2\tau}{\varepsilon}\partial_x\right)\beta\Pi_+\right]\left(u(t_n)-u^n\right)\right\|_r.$$

Considering the function $\varphi_1(\cdot)$, we write

$$|\varphi_1(ix)|=\frac{|\cos x-1+i\sin x|}{|x|}\le\left|\frac{\cos x-1}{x}\right|+\left|\frac{\sin x}{x}\right|\le 2\quad\text{for all}\quad x\in\mathbb{R},\quad x\ne 0,$$

and $\varphi(0)=1$. Since $\beta$ is isometric and $\Pi_\pm$ are projectors, we obtain

$$\left\|I_1(t_n,\tau)-I_1^n\right\|_r \le 2\tau\delta\left\|u(t_n)-u^n\right\|_r \le C\tau\left\|e^n\right\|_r. \tag{5.13}$$

Analogously, subtracting (5.9) from (5.6) and taking into account assumption (A) implies

$$\begin{aligned}\left\|I_2(t_n,\tau)-I_2^n\right\|_r &= \tau\left\|\left[\left(\varphi_1\left(\frac{\tau}{\varepsilon}\partial_x\right)V\right)\Pi_+ + \left(\varphi_1\left(-\frac{\tau}{\varepsilon}\partial_x\right)V\right)\Pi_-\right](u(t_n)-u^n)\right\|_r \\ &\le C\tau\left\|e^n\right\|_r. \end{aligned}\tag{5.14}$$

In order to estimate $\|I_3(t_n,\tau)-I_3^n\|_r$, we have to assume that the numerical solution $u^n$ is bounded. For $n=0$ it follows from assumption (B), since

$$\|u^0\|_r = \|u(0,x)\|_r \le \|u\|_{L^\infty([0,T];(H^r)^2)}.$$

We complete the estimates by mathematical induction. Assuming that the estimate

$$\|u^n\|_r \le \|u\|_{L^\infty([0,T];(H^r)^2)} + 1 \tag{5.15}$$

is true for all $0\le n\le m<T/\tau$, we justify it for $n=m+1$ and then estimate $\|I_3(t_n,\tau)-I_3^n\|_r$ for $n\le m$. Subtracting (5.9) from (5.7), and using the triangle inequality and (5.15) gives

$$\begin{aligned}\left\|I_3(t_n,\tau)-I_3^n\right\|_r &\le C\tau\left(\|u_+(t_n)-u_+^n\|_r + \|u_-(t_n)-u_-^n\|_r\right) \\ &\le C\tau\left\|e^n\right\|_r, \quad 0\le n\le m. \end{aligned}\tag{5.16}$$

Combining (5.10)-(5.14), and (5.16) leads to the inequality

$$\|\mathrm{e}^{n+1}\|_r \le \|\mathrm{e}^n\|_r + C\tau\|\mathrm{e}^n\|_r + C\tau^2, \quad 0\le n\le m.$$

Applying the discrete Gronwall's inequality, we get

$$\|\mathrm{e}^{m+1}\|_r \le C\tau$$

for a constant $C>0$ depending on $T$ and $\|u\|_{L^\infty([0,T];(H^r)^2)}$. Hence, for a sufficiently small positive $\tau$, the triangle inequality leads to the estimate

$$\|u^{m+1}\|_r \le \|\mathrm{e}^{m+1}\|_r + \|u\|_{L^\infty([0,T];(H^r)^2)} \le \|u\|_{L^\infty([0,T];(H^r)^2)} + 1,$$

which completes the proof of Theorem 5.1. □

**Remark 5.1.** We remark that the assumption $r>1/2$ in Theorem 5.1 is necessary to apply classical bilinear estimates in the error analysis — i.e. in this case we exploit the fact that $H^r$ is an algebra. This stability restriction can be eased by using discrete Strichartz-type estimates — cf. [36].

The above theorem shows the first-order accuracy of UA (5.8)-(5.9) for all $\varepsilon\in(0,1]$ without imposing restrictions on the time-step size.

## 6. Numerical Results

In this section, we carry out numerical experiments and compare the performance of the numerical methods under consideration. We solve the nonlinear Dirac equation (1.1) in massless nonrelativistic regime on $\mathbb{T}=(-\pi,\pi)$ with $\delta=1$, $\lambda=1, V(x)=2\sin(x)$ and the initial data

$$u_0(x)=\left(\frac{\sin(x)}{2+\cos(x)^2},\frac{\cos(x)}{2+\sin(x)}\right)^T,\quad x\in\mathbb{T}.$$

For the spatial discretization, we apply the Fourier pseudospectral method [41, 44]. Let $u^n_{h,\tau}$ be the numerical solution obtained by using the mesh of a size $h$ and a time-step size $\tau$ at the time $t_n=n\tau, n=0,1,\ldots$. To evaluate the convergence, we define the numerical error as

$$\text{error} := e_{h,\tau}=\left\|u(t_n,\cdot)-u^n_{h,\tau}\right\|_{l^2}=\sqrt{h\sum_{j=0}^{N-1}\left|u(t_n,x_j)-(u^n_{h,\tau})_j\right|^2},$$

where $N=2\pi/h$ is the number of grid points, $x_j=-\pi+hj$, and $u(t_n,x)$ the reference solution obtained numerically by fine mesh and time-steps — viz. $h=2\pi/2^8, \tau=2^{-18}$.

We first illustrate the spatial error of the numerical methods. To neglect the temporal error, the time-step size is set to $\tau=2^{-18}$ for all methods. Fig. 2 shows the spatial errors at $t_n=T=0.5$ for $\varepsilon=1$ and $\varepsilon=2^{-12}$. Note that for both values of $\varepsilon$ all methods are spectral accurate in space and the errors change a little if $h\le 2\pi/2^6\approx 0.1$.

After that we mainly focus on temporal convergence. Based on the above spatial error convergence test, we now fix the mesh size $h=2\pi/2^8$, so that the spatial error is negligible compared to the temporal error. We also take $t_n=0.5$ as the terminate time. The reference solutions are obtained by the Strang splitting method with $h=2\pi/2^8, \tau=2^{-18}$.

Fig. 3 and Tables 1-2 show the temporal errors of semi-implicit finite difference methods for different $\varepsilon$ and $\tau$. As is shown Fig. 3(a), SIFD1 is linearly convergent when $\varepsilon=1$,

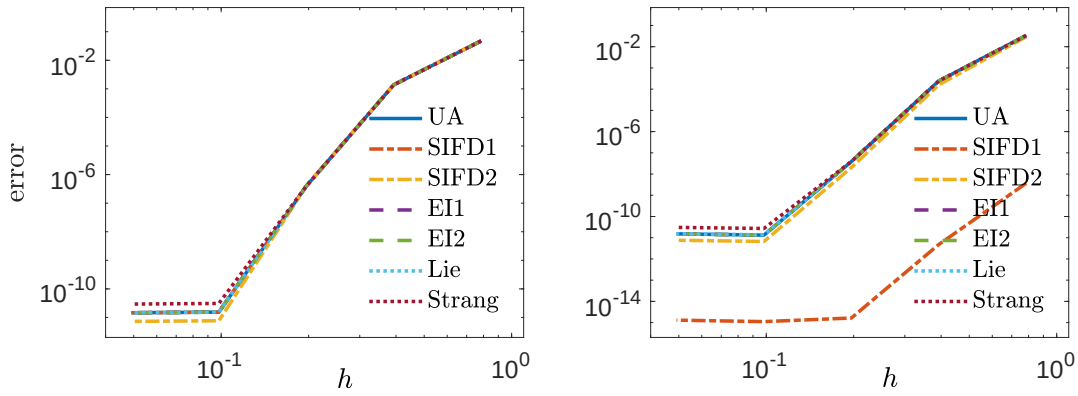


Figure 2: Spatial errors of different methods. Left: $\varepsilon=1$. Right: $\varepsilon=2^{-12}$.

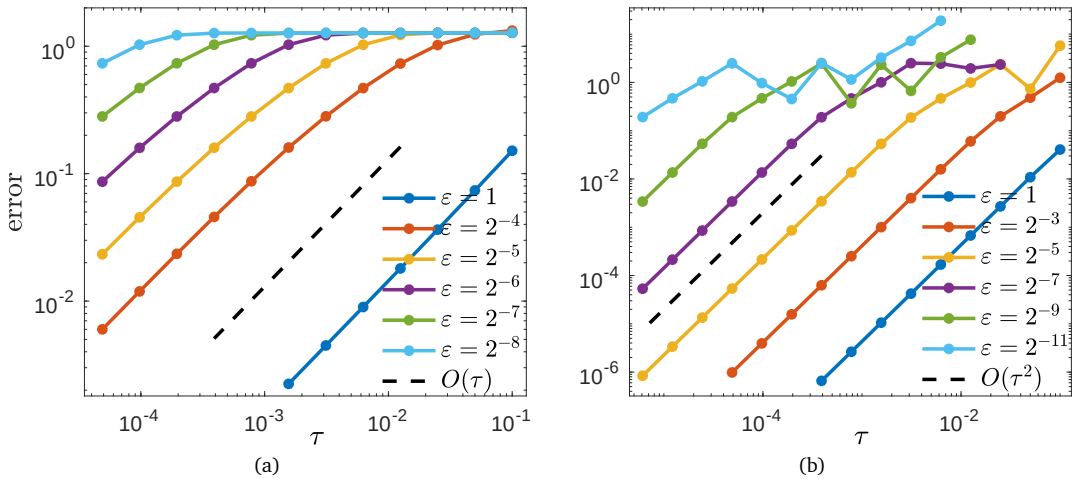


Figure 3: Temporal error analysis at $t_n = 0.5$. (a) SIFD1. (b) SIFD2.

while order reduction occurs as $\varepsilon$ becomes smaller. It is clearly seen that SIFD1 is not optimally convergent until $\tau$ got smaller than the $\varepsilon$-dependent $\tau_0$, i.e. $\tau \le \tau_0(\varepsilon)$. Table 1 demonstrates the relationship between $\tau_0(\varepsilon)$ and $\varepsilon$ more clearly. In particular, SIFD1 is only linearly convergent in the upper triangle part, and the bold diagonal part implies that $\tau_0(\varepsilon)$ is divided by 4 as $\varepsilon$ is divided by 2, i.e. $\tau_0(\varepsilon) = C\varepsilon^2$. That is, SIFD1 is linearly convergent only when $\tau \le C\varepsilon^2$. Fig. 3(b) and Table 2 also show the order reduction for SIFD2, and imply that SIFD2 is quadratically convergent only if $\tau \le C\varepsilon^{3/2}$. Thus numerical results for the semi-implicit finite difference methods match the analysis in Section 2.

Table 1: Temporal error analysis of SIFD1. The convergence order is obtained by $\log_4(e_{h,4\tau}/e_{h,\tau})$.

| error | $\tau = 0.1$ | $\tau = 0.1/4$ | $\tau = 0.1/4^2$ | $\tau = 0.1/4^3$ | $\tau = 0.1/4^4$ | $\tau = 0.1/4^5$ |
|---|---|---|---|---|---|---|
| $\varepsilon = 1$ | 1.51E-01 | **3.64E-02** | 8.98E-03 | 2.24E-03 | 5.59E-04 | 1.40E-04 |
| Order | - | **1.03** | 1.01 | 1.00 | 1.00 | 1.00 |
| $\varepsilon = 2^{-1}$ | 1.95E-01 | 5.34E-02 | **1.37E-02** | 3.46E-03 | 8.67E-04 | 2.17E-04 |
| Order | - | 0.93 | **0.98** | 0.99 | 1.00 | 1.00 |
| $\varepsilon = 2^{-2}$ | 4.66E-01 | 1.72E-01 | 5.04E-02 | **1.32E-02** | 3.34E-03 | 8.38E-04 |
| Order | - | 0.72 | 0.89 | **0.97** | 0.99 | 1.00 |
| $\varepsilon = 2^{-3}$ | 1.02 | 4.84E-01 | 1.71E-01 | 4.97E-02 | **1.30E-02** | 3.29E-03 |
| Order | - | 0.54 | 0.75 | 0.89 | **0.97** | 0.99 |
| $\varepsilon = 2^{-4}$ | 1.33 | 1.02 | 4.69E-01 | 1.60E-01 | 4.57E-02 | **1.19E-02** |
| Order | - | 0.19 | 0.56 | 0.77 | 0.90 | **0.97** |
| $\varepsilon = 2^{-5}$ | 1.28 | 1.28 | 1.03 | 4.70E-01 | 1.60E-01 | 4.54E-02 |
| Order | - | 0.00 | 0.16 | 0.56 | 0.78 | 0.91 |
| $\varepsilon = 2^{-6}$ | 1.28 | 1.27 | 1.27 | 1.03 | 4.70E-01 | 1.59E-01 |
| Order | - | 0.00 | 0.00 | 0.15 | 0.56 | 0.78 |

Table 2: Temporal error analysis of SIFD2. The convergence order is obtained by $\log_8(e_{h,8\tau}/e_{h,\tau})$.

| error | $\tau=0.1$ | $\tau=0.1/8$ | $\tau=0.1/8^2$ | $\tau=0.1/8^3$ | $\tau=0.1/8^4$ |
|---|---|---|---|---|---|
| $\varepsilon=2^{-1}$ | 1.17E-01 | **1.55E-03** | 2.42E-05 | 3.78E-07 | 5.92E-09 |
| Order | - | **2.08** | 2.00 | 2.00 | 2.00 |
| $\varepsilon=2^{-3}$ | 1.25 | 6.02E-02 | **1.01E-03** | 1.57E-05 | 2.46E-07 |
| Order | - | 1.46 | **1.97** | 2.00 | 2.00 |
| $\varepsilon=2^{-5}$ | 5.76 | 9.95E-01 | 5.34E-02 | **8.61E-04** | 1.34E-05 |
| Order | - | 0.84 | 1.41 | **1.99** | 2.00 |
| $\varepsilon=2^{-7}$ | 1.64E+36 | 1.95 | 1.00 | 5.35E-02 | **8.53E-04** |
| Order | - | 39.78 | 0.32 | 1.41 | **1.99** |
| $\varepsilon=2^{-9}$ | 2.95E+84 | 7.67 | 2.33 | 1.05 | 5.35E-02 |
| Order | - | 92.55 | 0.57 | 0.39 | 1.43 |

Fig. 4 and Tables 3-4 show the temporal errors and convergence order of the exponential integrators. Similar to finite difference methods, the convergence of exponential integrators depends on $\varepsilon$. Both EI1 and EI2 achieve optimal convergence orders only if $\tau \le C\varepsilon$. This also validate our analysis in Section 4.

For splitting methods, numerical results are a little different and surprising. As is shown in Figs. 5-6, the order reduction indeed exists and $\varepsilon$-dependence is consistent with the analysis in Section 3, i.e. an optimal convergence is achieved if $\tau \le C\varepsilon$. Unlike to the two methods above, the maximum errors over different $\varepsilon$ in two figures keep decreasing as $\tau$ goes smaller. This suggests that the splitting methods may also be uniformly convergent. Super-resolution and improved error bounds of the splitting methods have also been found and analyzed for Dirac and nonlinear Dirac equations in the nonrelativistic regime [6, 7], and for the highly oscillatory nonlinear Schrödinger equation [18]. It should be also analysed in the massless nonrelativistic regime.

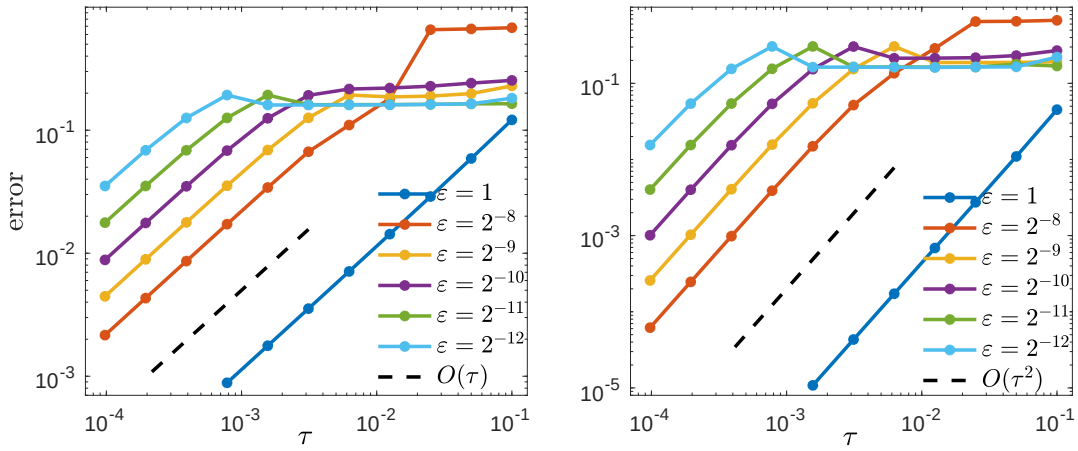


Figure 4: Temporal error analysis at $t_n = 0.5$. Left: EI1. Right: EI2.

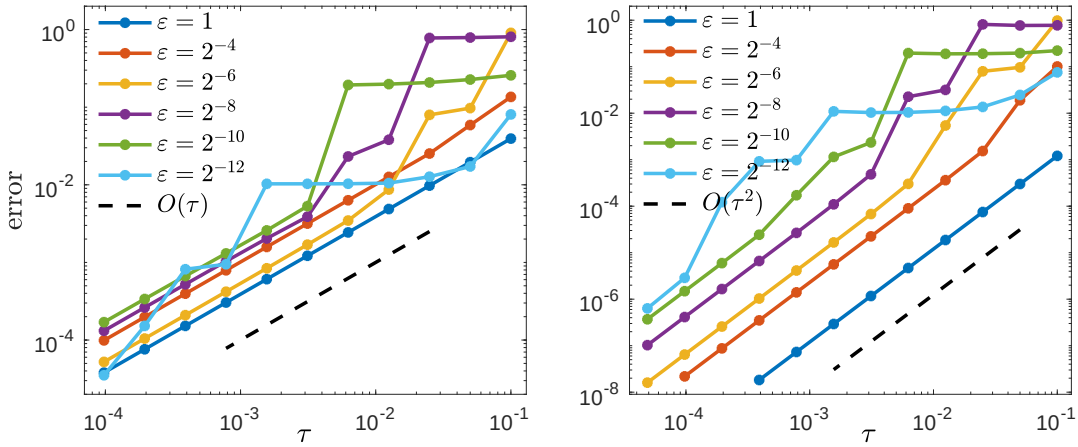


Figure 5: Temporal error analysis at $t_n = 0.5$. Left: Lie-Trotter splitting. Right: Strang splitting.

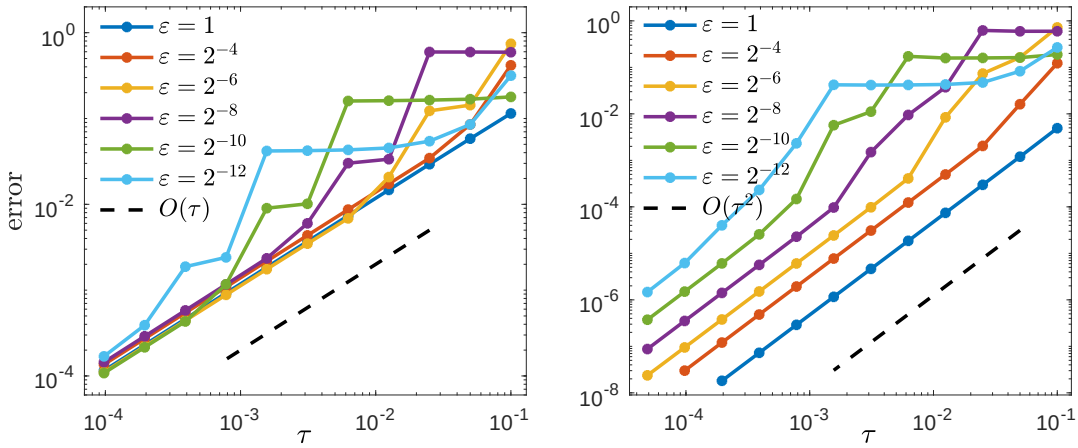


Figure 6: Temporal error analysis at $t_n = 5$. Left: Lie-Trotter splitting. Right: Strang splitting.

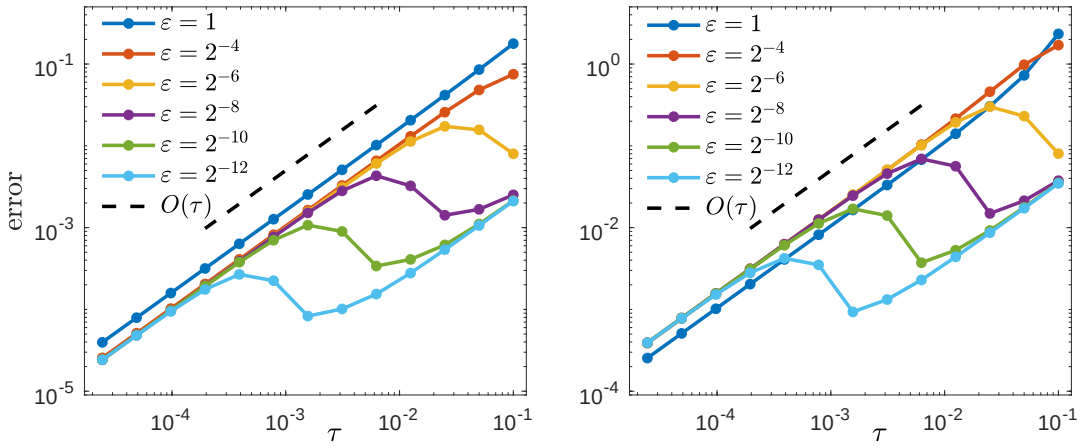


Figure 7: Temporal error analysis of uniformly accurate method. Left: $t_n = 0.5$. Right: $t_n = 5$.

Table 3: Temporal error analysis of EI1. The convergence order is obtained by $\log_4(e_{h,4\tau}/e_{h,\tau})$.

| error | $\tau = 0.1/4$ | $\tau = 0.1/4^2$ | $\tau = 0.1/4^3$ | $\tau = 0.1/4^4$ | $\tau = 0.1/4^5$ | $\tau = 0.1/4^6$ |
|---|---|---|---|---|---|---|
| $\varepsilon = 2^{-2}$ | 3.19E-02 | 7.81E-03 | 1.94E-03 | 4.85E-04 | 1.21E-04 | 3.03E-05 |
| Order | - | 1.01 | 1.00 | 1.00 | 1.00 | 1.00 |
| $\varepsilon = 2^{-4}$ | 2.94E-02 | **7.30E-03** | 1.82E-03 | 4.55E-04 | 1.14E-04 | 2.84E-05 |
| Order | - | **1.01** | 1.00 | 1.00 | 1.00 | 1.00 |
| $\varepsilon = 2^{-6}$ | 8.54E-02 | 3.43E-02 | **8.61E-03** | 2.15E-03 | 5.38E-04 | 1.34E-04 |
| Order | - | 0.66 | **1.00** | 1.00 | 1.00 | 1.00 |
| $\varepsilon = 2^{-8}$ | 6.56E-01 | 1.10E-01 | 3.42E-02 | **8.63E-03** | 2.16E-03 | 5.40E-04 |
| Order | - | 1.29 | 0.84 | **0.99** | 1.00 | 1.00 |
| $\varepsilon = 2^{-10}$ | 2.28E-01 | 2.16E-01 | 1.25E-01 | 3.50E-02 | **8.82E-03** | 2.21E-03 |
| Order | - | 0.04 | 0.39 | 0.92 | **0.99** | 1.00 |
| $\varepsilon = 2^{-12}$ | 1.62E-01 | 1.61E-01 | 1.60E-01 | 1.26E-01 | 3.52E-02 | **8.87E-03** |
| Order | - | 0.01 | 0.00 | 0.18 | 0.92 | **0.99** |

Table 4: Temporal error analysis of EI2. The convergence order is obtained by $\log_4(e_{h,4\tau}/e_{h,\tau})$.

| error | $\tau = 0.1/4$ | $\tau = 0.1/4^2$ | $\tau = 0.1/4^3$ | $\tau = 0.1/4^4$ | $\tau = 0.1/4^5$ | $\tau = 0.1/4^6$ |
|---|---|---|---|---|---|---|
| $\varepsilon = 2^{-2}$ | 5.56E-03 | 3.46E-04 | 2.16E-05 | 1.35E-06 | 8.44E-08 | 5.28E-09 |
| Order | - | 2.00 | 2.00 | 2.00 | 2.00 | 2.00 |
| $\varepsilon = 2^{-4}$ | 1.42E-02 | **9.44E-04** | 5.98E-05 | 3.75E-06 | 2.34E-07 | 1.46E-08 |
| Order | - | **1.95** | 1.99 | 2.00 | 2.00 | 2.00 |
| $\varepsilon = 2^{-6}$ | 1.05E-01 | 1.43E-02 | **9.34E-04** | 5.86E-05 | 3.67E-06 | 2.29E-07 |
| Order | - | 1.44 | **1.97** | 2.00 | 2.00 | 2.00 |
| $\varepsilon = 2^{-8}$ | 6.48E-01 | 1.36E-01 | 1.49E-02 | **9.85E-04** | 6.18E-05 | 3.87E-06 |
| Order | - | 1.13 | 1.59 | **1.96** | 2.00 | 2.00 |
| $\varepsilon = 2^{-10}$ | 2.17E-01 | 2.14E-01 | 1.53E-01 | 1.54E-02 | **1.01E-03** | 6.35E-05 |
| Order | - | 0.01 | 0.24 | 1.66 | **1.96** | 2.00 |
| $\varepsilon = 2^{-12}$ | 1.64E-01 | 1.63E-01 | 1.63E-01 | 1.55E-01 | 1.55E-02 | **1.02E-03** |
| Order | - | 0.01 | -0.00 | 0.04 | 1.66 | **1.97** |

Temporal errors of the uniformly accurate method are shown Fig. 7 with $t_n = 0.5$ and $t_n = 5$ for different $\varepsilon$. Note that for a fixed $\varepsilon$ the UA method is linearly convergent if $\tau$ is either small or large enough. There also exists convergence order degeneration. However, unlike to the above methods, this degeneration does not affect the uniform convergence of the UA method. Besides, the error does not apparently increases as $\varepsilon$ decreases and the UA method is still linearly convergent when taking the maximum error over all $\varepsilon$. Therefore, the UA method is uniformly linearly convergent for all $\varepsilon \in (0, 1]$.

Overall, in the massless nonrelativistic regime, the splitting and UA methods are more accurate than the others. According to Figs. 5-7, the UA method seems to have advantage

over splitting methods, since when $\tau$ is large the error for a small $\varepsilon$ in Fig. 7 is much smaller than a large $\varepsilon$ case ($\varepsilon = 1$ or $\varepsilon = 2^{-4}$), while the situation in Figs. 5 and 6 is just opposite. But if the Strang splitting method has an improve error estimate as in [6, 7], it may have a better performance with nonresonant time-step sizes.

## 7. Conclusion

We considered numerical methods for the nonlinear Dirac equation in the massless nonrelativistic regime. The model equation contains a small dimensionless parameter $0 < \varepsilon \leq 1$, which is inversely proportional to the speed of light, and the solution is highly oscillatory in time with wavelength $\mathcal{O}(\varepsilon)$. Investigating popular numerical schemes such as finite difference, time-splitting, and exponential integrator methods, we found that they all suffer from convergence order reduction problems when $0 < \varepsilon \ll 1$. Therefore, we proposed a uniformly accurate method, which always converges at an optimal rate without restrictions on the time-step size. Numerical experiments validate our analysis and illustrate the advantage of the UA method.

## Acknowledgments

We would like to thank Prof. Xiaofei Zhao for the helpful discussions.

This work was supported by NSFC (Grants 12125103, 12071362, 12001221), by the National Key Research and Development Program of China (Grant 2020YFA0714200), and by the Natural Science Foundation of Hubei Province (Grant 2019CFA007).

## References

[1] M. Ablowitz and Y. Zhu, *Nonlinear waves in shallow honeycomb lattices*, SIAM J. Appl. Math. **72**, 240–260 (2012).

[2] A. Alvarez and B. Carreras, *Interaction dynamics for the solitary waves of a nonlinear Dirac model*, Phys. Lett. **86**, 327–332 (1981).

[3] W. Bao, Y. Cai, X. Jia and Q. Tang, *A uniformly accurate multiscale time integrator pseudospectral method for the Dirac equation in the nonrelativistic limit regime*, SIAM J. Numer. Anal. **54**, 1785–1812 (2016).

[4] W. Bao, Y. Cai, X. Jia and Q. Tang, *Numerical methods and comparison for the Dirac equation in the nonrelativistic limit regime*, J. Sci. Comput. **71**, 1094–1134 (2017).

[5] W. Bao, Y. Cai, X. Jia and J. Yin, *Error estimates of numerical methods for the nonlinear Dirac equation in the nonrelativistic limit regime*, Sci. China Math. **59**, 1461–1494 (2016).

[6] W. Bao, Y. Cai and J. Yin, *Super-resolution of time-splitting methods for the Dirac equation in the nonrelativistic limit regime*, Math. Comp. **89**, 2141–2173 (2020).

[7] W. Bao, Y. Cai and J. Yin, *Uniform error bounds of time-splitting methods for the nonlinear Dirac equation in the nonrelativistic regime without magnetic potential*, SIAM J. Numer. Anal. **59**, 1040–1066 (2021).

[8] W. Bao, Y. Cai and X. Zhao, *A uniformly accurate multiscale time integrator pseudospectral method for the Klein-Gordon equation in the nonrelativistic limit regime*, SIAM J. Numer. Anal. **52**, 2488–2511 (2014).

[9] W. Bao, X. Dong and X. Zhao, *Uniformly accurate multiscale time integrators for highly oscillatory second order differential equations*, J. Math. Study. **47**, 111–150 (2014).
[10] W. Bao and J. Yin, *A fourth-order compact time-splitting Fourier pseudospectral method for the Dirac equation*, Res. Math. Sci. **6**, 11–35 (2019).
[11] W. Bao and X. Zhao, *A uniformly accurate (UA) multiscale time integrator Fourier pseudospectral method for the Klein-Gordon-Schrödinger equations in the nonrelativistic limit regime*, Numer. Math. **135**, 833–873 (2017).
[12] S. Baumstark, E. Faou and K. Schratz, *Uniformly accurate exponential-type integrators for Klein-Gordon equations with asymptotic convergence to the classical NLS splitting*, Math. Comp. **87**, 1227–1254 (2018).
[13] J. Bolte and S. Keppeler, *A semiclassical approach to the Dirac equation*, Ann. Phys. **274**, 125–162 (1999).
[14] Y. Cai and Y. Wang, *A uniformly accurate (UA) multiscale time integrator pseudospectral method for the nonlinear Dirac equation in the nonrelativistic limit regime*, ESAIM. Math. Model. **52**, 543–566 (2018).
[15] Y. Cai and Y. Wang, *Uniformly accurate nested Picard iterative integrators for the Dirac equation in the nonrelativistic limit regime*, SIAM J. Numer. Anal. **57**, 1602–1624 (2019).
[16] Y. Cai and Y. Wang, *Uniformly accurate nested Picard iterative integrators for the nonlinear Dirac equation in the nonrelativistic regime*, Multiscale Model. Sim. **20**, 164–187 (2022).
[17] P. Chartier, N. Crouseilles, M. Lemou and F. Méhats, *Uniformly accurate numerical schemes for highly oscillatory Klein-Gordon and nonlinear Schrödinger equations*, Numer. Math. **129**, 211–250 (2015).
[18] P. Chartier, F. Méhats, M. Thalhammer and Y. Zhang, *Improved error estimates for splitting methods applied to highly-oscillatory nonlinear Schrödinger equations*, Math. Comp. **85**, 2863–2885 (2016).
[19] N. Crouseilles, M. Lemou and F. Méhats, *Asymptotic preserving schemes for highly oscillatory Vlasov-Poisson equations*, J. Comp. Phys. **248**, 287–308 (2013).
[20] N. Crouseilles, M. Lemou, F. Méhats and X. Zhao, *Uniformly accurate forward semi-Lagrangian methods for highly oscillatory Vlasov-Poisson equations*, SIAM J. Multiscale Model. Sim. **15**, 723–744 (2017).
[21] P.A.M. Dirac, *The quantum theory of the electron*, Proc. R. Soc. Lond. A. **117**, 610–624 (1928).
[22] P.A.M. Dirac, *Principles of Quantum Mechanics*, Oxford University Press (1958).
[23] C.L. Fefferman and M.I. Weistein, *Honeycomb lattice potentials and Dirac points*, J. Amer. Math. Soc. **25**, 1169–1220 (2012).
[24] L.L. Foldy and S.A. Wouthuysen, *On the Dirac theory of spin 1/2 particles and its non-relativistic limit*, Phys. Rev. **78**, 29–36 (1950).
[25] D.J. Gross and A. Neveu, *Dynamical sysmmetry breaking in asymptotically free field theories*, Phys. Rev. D. **10**, 3235–3253 (1974).
[26] L.H. Haddad and L.D. Carr, *The nonlinear Dirac equation in Bose-Einstein condensates: Superfluid fluctuations and emergent theories from relativistic linear stability equations*, New J. Phys. **17**, 093037 (2015).
[27] R. Hammer, W. Pötz and A. Arnold, *Single-cone real-space finite difference scheme for the timedependent Dirac equation*, J. Comput. Phys. **265**, 50–70 (2014).
[28] H. Hasegawa, *Bound states of the one-dimensional Dirac equation for scalar and vector double square-well potentials*, Physica E **59**, 192–201 (2014).
[29] M. Hochbruck and A. Ostermann, *Exponential integrators*, Acta Numer. **19**, 209–286 (2000).
[30] D.D. Ivanenko, *Notes to the theory of interaction via particles*, Zhurn. Exp. Teoret. Fiz. **8**, 260–266 (1938).

[31] T.W.B. Kibble, *Lorentz invariance and the gravitational field*, J. Math. Phys. **2**, 212–221 (1961).
[32] P. Krämer, K. Schratz and X. Zhao, *Splitting methods for nonlinear Dirac equations with Thirring type interaction in the nonrelativistic limit regime*, J. Comput. Appl. Math. **387**, 112494 (2021).
[33] M. Lemou, F. Méhats and X. Zhao, *Uniformly accurate numerical schemes for the nonlinear Dirac equation in the nonrelativistic limit regime*, Commun. Math. Sci. **15**, 1107–1128 (2017).
[34] Y. Ma and J. Yin, *Error bounds of the finite difference time domain methods for the Dirac equation in the semiclassical regime*, J. Sci. Comput. **81**, 1801–1822 (2019).
[35] R.I. Mclachlan and G.R.W. Quispel, *Splitting methods*, Acta Numer. **11**, 341–434 (2002).
[36] A. Ostermann, F. Rousset and K. Schratz, *Error estimates of a Fourier integrator for the cubic Schrödinger equation at low regularity*, Found. Comput. Math. **21**, 725–765 (2021).
[37] W. Pötz, *Single-cone finite-difference schemes for the (2+1)-dimensional Dirac equation in general electromagnetic textures*, Phys. Rev. E. **96**, 053312 (2017).
[38] K. Schratz, Y. Wang and X. Zhao, *Low-regularity integrators for nonlinear Dirac equations*, Math. Comput. **90**, 189–214 (2021).
[39] S. Shao and H. Tang, *Interaction for the solitary waves of a nonlinear Dirac model*, Phys. Lett. A. **345**, 119–128 (2005).
[40] S. Shao and H. Tang, *Higher-order accurate Runge-Kutta discontinuous Galerkin methods for a nonlinear Dirac model*, Discrete Cont. Dyn. Syst. B. **6**, 623–640 (2006).
[41] J. Shen, T. Tang and L. Wang, *Spectral Methods: Algorithms, Analysis and Applications*, Springer (2011).
[42] T. Tao, *Nonlinear Dispersive Equations: Local and Global Analysis*, AMS (2006).
[43] W.E. Thirring, *A soluble relativistic field theory*, Ann. Physics. **3**, 91–112 (1958).
[44] L.N. Trefethen, *Spectral Methods in MATLAB*, SIAM (2000).
[45] H. Wu, Z. Huang, S. Jin and D. Yin, *Gaussian beam methods for the Dirac equation in the semiclassical regime*, Comm. Math. Sci. **10**, 1301–1315 (2012).
[46] J. Xu, S. Shao and H. Tang, *Numerical methods for nonlinear Dirac equation*, J. Comput. Phys. **245**, 131–149 (2013).